PLOS ONE

Hyaluronic acid on the urokinase sustained release with a hydrogel system composed of poloxamer 407: HA/P407 hydrogel system for drug delivery

Hao-Ying Hsieh[1]ʘ, Wei-Yang Lin[1,2]ʘ, An Li Lee[1,3], Yi-Chen Li[4], Yi-Jane Chen[5], Ke-Cheng Chen[1,6]*, Tai-Horng Young[ORCID][1]*

1 Department of Biomedical Engineering, National Taiwan University, Taipei, Taiwan, 2 Department of Thoracic Surgery, Lo-Hsu Medical Foundation, Lotung Poh-Ai Hospital, Lotung, Taiwan, 3 Division of Plastic Surgery, Department of Surgery, Mackay Memorial Hospital, Taipei, Taiwan, 4 Department of Chemical Engineering, Feng Chia University, Taichung, Taiwan, 5 Department of Dentistry, National Taiwan University Hospital, Taipei, Taiwan, 6 Department of Surgery, National Taiwan University Hospital, Taipei, Taiwan

ʘ These authors contributed equally to this work.
* cskchen@gmail.com (KCC); thyoung@ntu.edu.tw (THY)

Abstract

Pleural empyema is an inflammatory condition characterized by accumulation of pus inside the pleural cavity, which is usually followed by bacterial pneumonia. During the disease process, the pro-inflammatory and pro-fibrotic cytokines in the purulent pleural effusion cause proliferation of fibroblasts and deposition of extracellular matrix, which lead to fibrin deposition and fibrothorax. Urokinase instillation therapy through a chest drainage tube is frequently used for fibrinolysis in patients with empyema. However, urokinase treatment requires multiple instillation (2–3 times per day, for 4–8 days) and easily flows out from the chest drainage tube due to its high water solubility. In this in vitro study, we developed a thermo-responsive hydrogel based on poloxamer 407 (P407) combined with hyaluronic acid (HA) for optimal loading and release of urokinase. Our results show that the addition of HA to poloxamer gels provides a significantly more compact microstructure, with smaller pore sizes (**$p < 0.001$). The differential scanning calorimetry (DSC) profile revealed no influence on the micellization intensity of poloxamer gel by HA. The 25% poloxamer-based gel was significantly superior to the 23% poloxamer-based gel, with slower gel erosion when comparing the 16th hour residual gel weight of both gels (*$p < 0.05$; **$p < 0.001$). The 25% poloxamer-HA gel also exhibited a superior urokinase release profile and longer release time. A Fourier-transform infrared spectroscopy (FT-IR) study of the P407/HA hydrogel showed no chemical interactions between P407 and HA in the hydrogel system. The thermoresponsive P407/HA hydrogel may have a promising potential in the loading and delivery of hydrophilic drugs. On top of that, in vitro toxicity test of this combination demonstrates a lower toxicity.

1. Introduction

Pleural empyema is an inflammatory condition characterized by accumulation of pus inside
the pleural cavity, which is usually followed by bacterial pneumonia [1]. Pleural effusion is
found in 9–30% of cases of bacterial pneumonia, 20% of which progress to empyema. The
pro-inflammatory and pro-fibrotic cytokines in the purulent pleural effusion cause the pro-
liferation of fibroblasts and deposition of extracellular matrix, which lead to fibrin deposi-
tion and fibrothorax [2]. Urokinase instillation therapy through a chest drainage tube is a
standard protocol used for fibrinolysis of the deposited fibrin material [3]. However, uroki-
nase treatment requires multiple instillation (2–3 times per day, for 4–8 days), and easily
flows out from the chest drainage tube due to its high water solubility [4, 5]. Therefore, we
attempted to develop a thermo-responsive hydrogel based on poloxamer 407 (P407) com-
bined with hyaluronic acid (HA) for the loading and release of urokinase and for over 24
hours.

P407 is a non-ionic tri-block copolymer composed of a central hydrophobic block of
polypropylene oxide sandwiched between two hydrophilic blocks of polyethylene oxide
(PEOx-PPOy-PEOx) [6]. P407 is a thermo-responsive polymer that is liquid at low tempera-
tures; and the aqueous polymer solution converts to a gel status when the temperature rises.
The solubility of the hydrophobic blocks decreases as they aggregate to minimize the inter-
action of PPO blocks with the solvent [7, 8]. Due to its thermo-responsive character, good
biocompatibility, and low toxicity [9], P407 is widely used for smart drug delivery [8] and
in different formulations such as nasal, ophthalmic, and vaginal [10–14]. When used on its
own, the P407 gel rapidly loses its gelation ability after dilution in a water-rich environment.
Blending P407 with other polymers or molecules for better drug loading and retention has
been previously studied [7, 8, 15]. For example, the P407 based hydrogels have been widely
used to encapsulate some small molecular drugs (with a molecular weight (MW) under
500g/mole) such as ketorolac, metoprolol, and doxycycline; and the P407-based hydrogels
could continually release these drugs for up to 20 hours [15, 16]. However, urokinase is a
hydrophilic macromolecular protein kinase with 411 amino acid residues and a molecular
weight of 32 kDa [17, 18], which facilitates the movement of water molecules into the uroki-
nase-loaded P407 gel and therefore faster dissolution of P407-based hydrogels due to the
larger constitutional property of urokinase, as shown in a previously reported *in vivo* study
[19]. Therefore, a proper additive is therefore needed in order to achieve an optimized
release of urokinase with the P407-based gel.

Hyaluronic acid (HA) is an endogenous glycosaminoglycan that exists in various tissues,
including connective tissues and the aqueous humor of the eye. This polysaccharide is com-
posed of disaccharide monomers (N-acetylglucosamine and glucuronic acid) and plays an
important role in tissue hydration, cell migration, and wound healing [20]. HA is highly
hydrophilic and able to form hydrogen bonds with water molecules. Also, HA was used as a
drug delivery agent with different routes of administration in ophthalmic, nasal, pulmonary
and oral [21], which has been reported to have the improved rheological and mucoadhesive
properties [22, 23]. In addition to the pure HA, HA/Poloxamer hydrogels were studied as a
thermo-responsive injectable filling material with the capability of controlled drug release for
bone regeneration [24]. However, those studies were devoted to chemical synthesis and formu-
lations. The release kinetics of urokinase and the effect of HA on urokinase-loaded drug
release system have not been reported yet. In this study, we investigated different combina-
tions of P407 and HA for the optimal effect of urokinase loading and release. Micellization and
gelation behavior, gel dissolution, release of urokinase and its stability within the gels, and gel
microstructure were also studied.

2. Materials and methods

2.1. Materials

In this study, we aimed to reduce the frequency to single administration daily at maximal in vivo regimen release. Poloxamer 407 (P407, culture tested) was obtained from Sigma-Aldrich (Gillingham, UK). Research-grade sodium hyaluronate (HA) of 490±11.3 kDa was purchased from Lifecore Biomedical, Inc. (Minnesota, USA). Lyophilized urokinase powder for injection (60000 IU) was purchased from Taiwan Green Cross Co., Ltd (Taiwan).

2.2. Sample preparation

23% and 25% w/w P407 aqueous solution was prepared using a 'cold method' [7, 8]. Briefly, a weighed amount of P407 was added to water that had been equilibrated at 4–8 ˚C before use. The poloxamer solution was then kept for a further 24–36 hours in a refrigerator until a clear solution was obtained. Under an ice bath (temperature maintained at 2–5 ˚C), 5, 6, or 7 mg of HA was added into every ml of 23% or 25% cold P407 aqueous solution for dissolution under gentle stirring for 2 h. Then, 60000 IU lyophilized urokinase was dissolved into 60 mL water to make a 1000 IU/mL aqueous solution. 100 IU urokinase (0.1 ml of 1000 IU/ml urokinase aqueous solution) was loaded into 1 mL of P407/HA solution on ice bath with gently stirred.

2.3. Fourier transform infrared spectroscopy (FT-IR)

Fourier-transform infrared spectroscopy (FT-IR) experiments were performed using a Spectrum 100 spectrometer (PerkinElmer, USA). The samples were previously ground and mixed thoroughly with potassium bromide (1 mg of sample to 80 mg of potassium bromide). Potassium bromide discs were prepared by compressing the powders in a hydraulic press. Scans were obtained at a resolution of 1 cm^{-1} from 4000 to 450 cm^{-1}.

2.4. Gel dissolution

Dissolution profiles of the P407-based gels in an aqueous environment were determined using the gravimetric method [25]. A pre-weighed glass vial of 13 mm diameter containing 0.6 g of the gel was equilibrated at 37 ˚C, and 0.3 mL of water previously equilibrated at 37 ˚C was layered over it. The liquid medium was removed at pre-determined time intervals, the vial was re-weighed, and the weight of residual gel was calculated from the difference in weight of the vial. The entire process was carried out in an incubation room maintained at 37 ˚C.

    In vitro cumulative release of urokinase. A membrane-less dissolution model was applied to the study of the release profile of urokinase [25]. The urokinase-loaded gels were treated as described above. The concentration of urokinase in the released medium was collected at pre-determined time intervals, and then determined using a fluorometric spectrophotometer utilizing the Abcam® Urokinase Fluorometric Activity Assay Kit (Abcam, USA). An AMC-based peptide substrate containing the recognition sequence for urokinase was used. The urokinase present in the sample catalyzes the cleavage of the substrate and releases AMC, which could be easily quantified by measuring its fluorescence at Ex/Em = 350/450 nm with an ELISA (SpectraMax M2, Molecular Devices, USA).

2.5. Differential scanning calorimetry (DSC)

Calorimetry was carried out using a MicroCal VP-DSC microcalorimeter (Malvern, USA) equipped with VP Viewer software. Approximately 5 mg of poloxamer aqueous solution was placed in sealed aluminum pans. Prior to measurement, the sample was subjected to the following thermal cycle: heating from 0 to 50 ˚C, then cooling from 50 to 0 ˚C at a rate of 10 ˚C/

min. DSC traces were then recorded as the temperature increased from 0 to 50˚C at a rate of 10 ˚C/min, with an empty pan as a reference. Data were analyzed to obtain onset temperature (T_{onset}), area under the peak, peak temperature (T_{peak}), and endset temperature (T_{endset}) of the endothermic peak.

2.6. Scanning electron microscope (SEM)

The samples were processed through lyophilization, which was used to preserve the cross-sections of samples. The samples were then coated with gold before being placed onto SEM specimen holders. The microstructures were observed under an S-4800 scanning electron microscope (Hitachi, Japan).

2.7. In vitro cytotoxicity

The cytotoxicity of 23% and 25% P407, urokinase and sodium hyaluronate were measured by Alamar blue assay. Normal fibroblasts (Hs68 cells) were seeded at a density of $2x10^4$ (cell/ml) per well in 1ml culture medium (DMEM-HG) supplemented with 10% FBS in a 48-well plate and incubated for 3 hours at 37˚C in a humidified incubator containing 5% CO_2. Urokinase concentrations tested were 1000(IU/ml)[26]. The P407: urokinase proportion was maintained at 9:1(ml) for all formulations into the cell culture wells, at final volume of 1 ml. Subsequently the Alamar blue fluorescence was quantified at excitation and emission wavelength of 560nm and 590nm respectively by ELISA plate reader. For each plate the reading was done in quadruplicate (n = 4)[27].

2.8. Statistical analysis

All tests in triplicate and repeated in three or more independent experiments. Representative data are expressed as mean ± standard deviation (SD). Statistical analysis was performed using SPSS 20.0 (SPSS Inc., Chicago. IL). Differences between experimental and control groups were analyzed by independent Student's t test. p-values $<0.05 = $ *, p $<0.001 = $ ** were considered statistically significant).

Results

3.1. FT-IR spectroscopy characterization

The FT-IR spectra of P407, HA, urokinase, and their physical mixtures (P407 + urokinase and P407 + HA + urokinase) were performed in order to investigate the molecular interactions between P407, HA, and urokinase. The P407 spectra revealed characteristic peaks of CH_2 stretch (2920 cm^{-1}), C-O stretch (1100 cm^{-1}), and C-O-C linkage (952 cm^{-1}). This was comparable with the previously recorded FT-IR spectra of P407 [16]. The HA spectra showed an absorption peak at 1732 cm^{-1}, corresponding to a C = O stretch. The spectra of the physical mixture (P407 + HA + urokinase) showed all the characteristic peaks of each chemicals without any shifts (Fig 1). Based on the FT-IR spectra, no chemical interactions between drug and polymer were observed in the physical mixtures.

3.2. Differential scanning calorimetry (DSC)

A DSC profile was used to determine the micellization behavior of P407 gels. The illustrative thermogram showed endothermic peaks indicative of micellization. The micellization process is characterized by the onset temperature (T_{onset}), the area under the peak that reflects the enthalpy change, the peak temperature (T_{peak}) [28], and the endset temperature (T_{endset}) [29]. T_{onset} is the temperature at which micelles begin to form, while T_{endset} is the temperature at
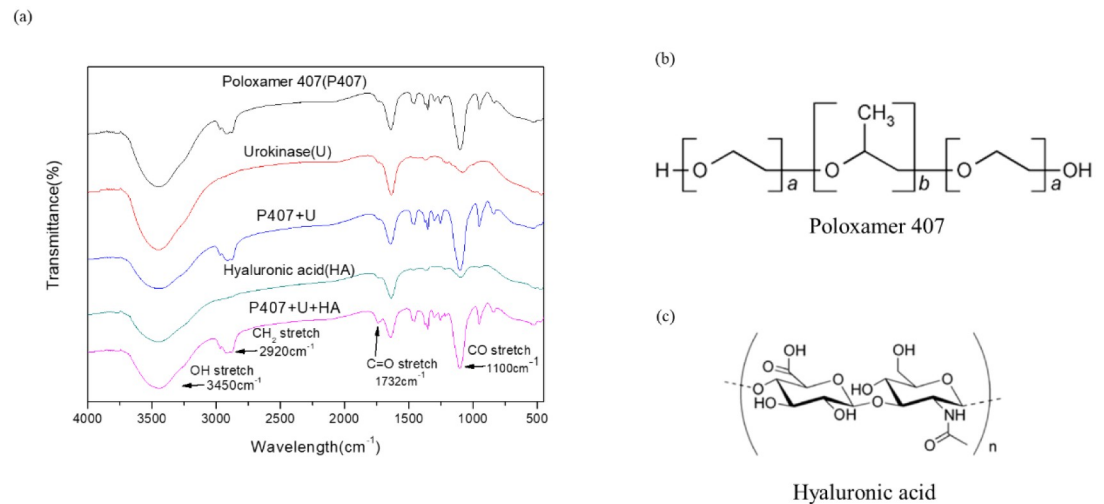
Fig 1. FT-IR spectra **(a)** of aqueous P407, U, P407+U, HA, and P407+U+HA. Chemical structure of **(b)** P407 and **(c)** HA.

which the micellization process is completed. The T_{peak} is referred to as the critical micellization temperature (CMT). The endothermic peak arises from the dehydration of the relatively hydrophobic polypropylene oxide (PPO) blocks of the P407 molecules during the micellization process, as previously reported [30].

The DSC thermogram showed a decrease in CMT when HA was added into pure 23% and 25% aqueous P407 solution (Fig 2). The micellization process occurred earlier in all aqueous P407/HA solutions as shown by the decrease in T_{onset}. The effect of added HA on micellization intensity is relatively minor. On the other hand, the addition of urokinase into aqueous P407 solution delayed the micellization process with a markedly decrease in the micellization intensity. This is demonstrated by the increase in T_{onset}, CMT, and T_{endset}, as well as the decrease in the endothermic peak (Fig 2c).

3.3. Dissolution of poloxamer gels

We examined the gel dissolution properties of pure P407 gels, P407 with HA, and P407 with HA and urokinase. The dissolution curve revealed no swelling of pure 23% P407 gel and a minor degree of swelling ($3.2 \pm 1.7\%$) of pure 25% P407 gel in the first hour. When HA was added into the P407 gels, a relatively wide degree of swelling ranging from $5.1 \pm 1.7\%$ to $17.5 \pm 4.7\%$ were observed in the first 3 hours. The degree of swelling increased with the increase of concentration of P407(23%, 25%) and HA (5.0mg/ml, 6.0mg/ml and 7.0mg/ml accordingly)(Fig 3a and 3b). The 25% P407 with 5mg/ml HA exhibited the highest degree of swelling ($17.5 \pm 4.7\%$). The addition of HA remarkably improved the hydrogel properties of pure P407 gels with extended gel dissolution time. When comparing the residual gel weights at 20th hour)(Fig 3c), the addition of HA significantly slowed down the gel erosion process in the 23% P407 gels. However, no statistically significant difference was observed between the 25% P407 and 25% P407+HA when comparing the residual gel weight at 24th hour)(Fig 3d).

Furthermore, the loading of urokinase into P407 gels accelerated the gel dissolution by 8–12 hours compared to pure P407 (Fig 4a and 4b). The addition of HA remarkably extended the gel erosion process in the urokinase-loaded 23% P407 when comparing the residual gel weights at 16th hour. Similarly, the extended gel erosion process was observed in the 25% P407 +HA+urokinase at 20th hour.
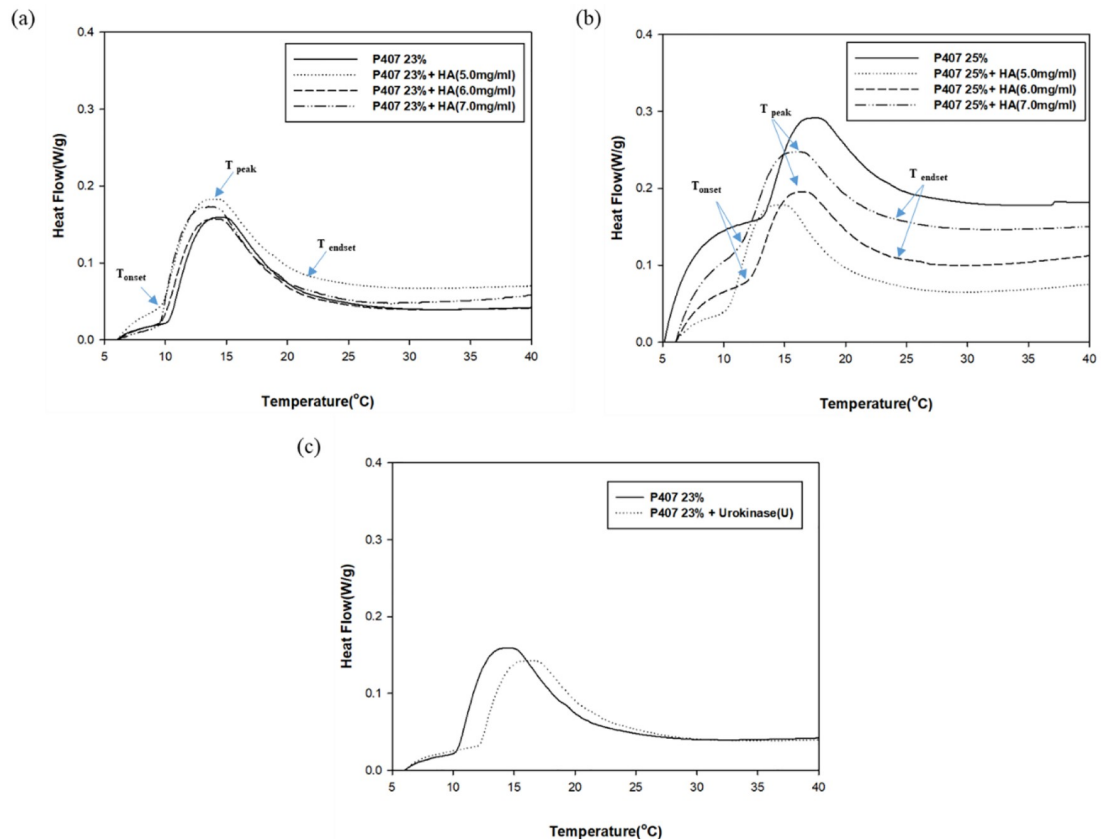
Fig 2. Micellization intensity P407-based gels. Tonset, CMT, and Tendset decreased when HA was added into the aqueous **(a)** 23% and **(b)** 25% P407. The influence of HA on micellization intensity was relatively minor. The micellization process was delayed and micellization intensity was decreased when **(c)** urokinase was added into aqueous P407 solution.

3.4. Release of urokinase from P407 gels

The release profiles of urokinase in the 23% P407 and 25% P407 was found to last for 20 hours and 24 hours, respectively (Fig 5). Moreover, the release of urokinase within the gels had been augmented in a significant rate by the addition of HA, which was reinforced in the scenario of 25% P407.

3.5. Microstructure of P407 gels influenced by the addition of urokinase and HA

SEM images showed the structures of pure P407 gels as porous and sponge-like. When urokinase was loaded into the P407 gels, a significant change in the structure and pore size was observed. However, the addition of HA significantly reduced the pore size and resulted in a more compact porous structure (Fig 6), suggesting the possible protective role of HA in this hydrogel system. The changed microstructural may explain the extended gel erosion we have observed, hence resulting in the higher stability of urokinase at 37°C.

3.6. In vitro cytotoxicity

The correlation between cytotoxicity and individual urokinase, sodium hyaluronate, (Fig 7a) 23% P407, (Fig 7b)25% P407 and their combination were assessed. The results showed that the
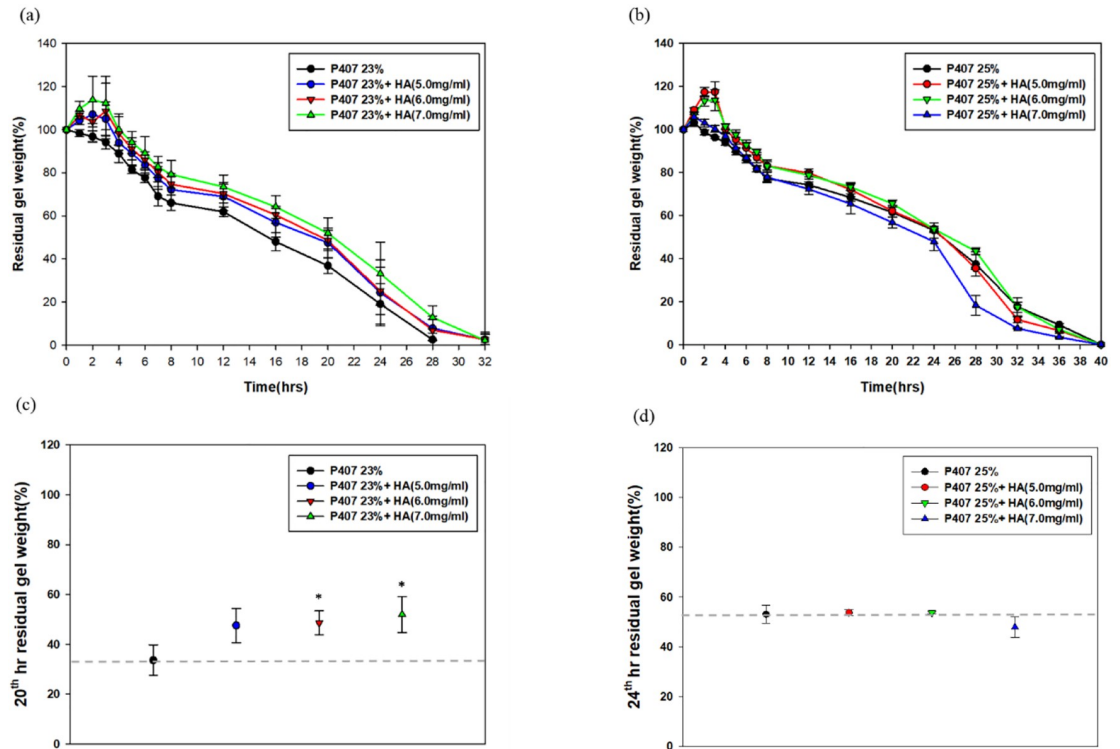
Fig 3. Gel dissolution profiles of (**a**) 23% and (**b**) 25% P407 with and without HA. The axis represents residual gel weight percentage at different time points. The addition of HA into 23% and 25% P407 gels markedly increases swelling rate in the first 3 hours. The addition of HA significantly slowed down the gel erosion in 23% and 25% P407 gels when compared at (**c**) 20th and (**d**) 24th hour, respectively. Significant differences from control group (P407+U) were denoted with $^*P < 0.05$ and $^{**}P < 0.01$.

https://doi.org/10.1371/journal.pone.0227784.g003

cellular activities of above materials were above 80% of the control. Based on the ISO10993-5 the grading of the test for in vitro cytotoxicity: Not more than 20% of the cells are round, loosely attached and without intracytoplasmatic granules, or show changes in morphology; occasional lysed cells are present; only slight growth inhibition observable. Therefore, in this study, the in vitro cytotoxicity of the material was low.
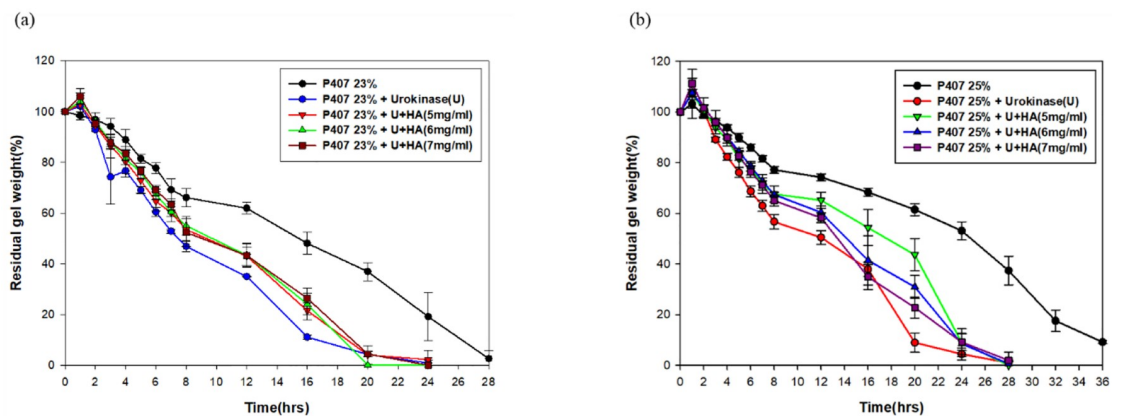

Fig 4. Gel dissolution profiles of (a) 23% and (b) 25% urokinase-loaded P407 with and without HA. The gel dissolution time decreased markedly in urokinase-loaded 23% and 25% P407 in the comparison with the non-urokinase-loaded gels.

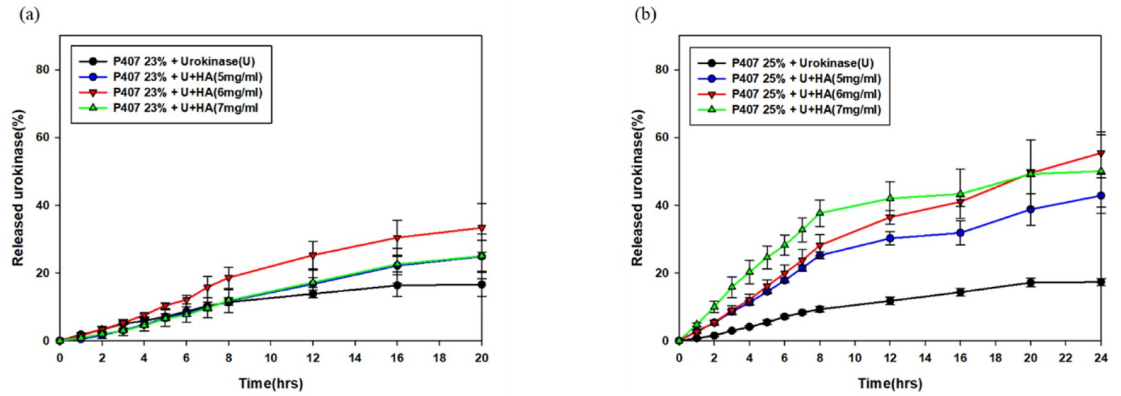https://doi.org/10.1371/journal.pone.0227784.g004

Fig 5. Urokinase release curves of 23% (a) and 25% (b) P407-based gels. The addition of HA into 25% P407 gel significantly increased urokinase activity.

https://doi.org/10.1371/journal.pone.0227784.g005

4. Discussion

P407, one of the members of the poly(PEOx-PPOy-PEOx) tri-block copolymers family, presents with a polyoxypropylene (PPO) molecular mass of 4,000 g/mol and a 70% polyoxyethylene (PEO) content. Both of the PEO and PPO blocks develop hydrogen bonds with water molecules, but the former is more hydrophilic than the latter. P407 is characterized by its temperature dependent self-assembling and thermo-gelling behavior. As the temperature rises, the aqueous P407 solution converts to a gel status driven by the decline of the solubility of PPO blocks, in which aggregation occurs in order to minimize their interaction with water molecules [7, 8]. The aggregated hydrophobic blocks comprise the core of the micelle, whilst the PEO blocks form the outer layer of hydrophilic shell that is bound to the water molecules covalently. The solution-to-gel transformation temperature is concentration-dependent and
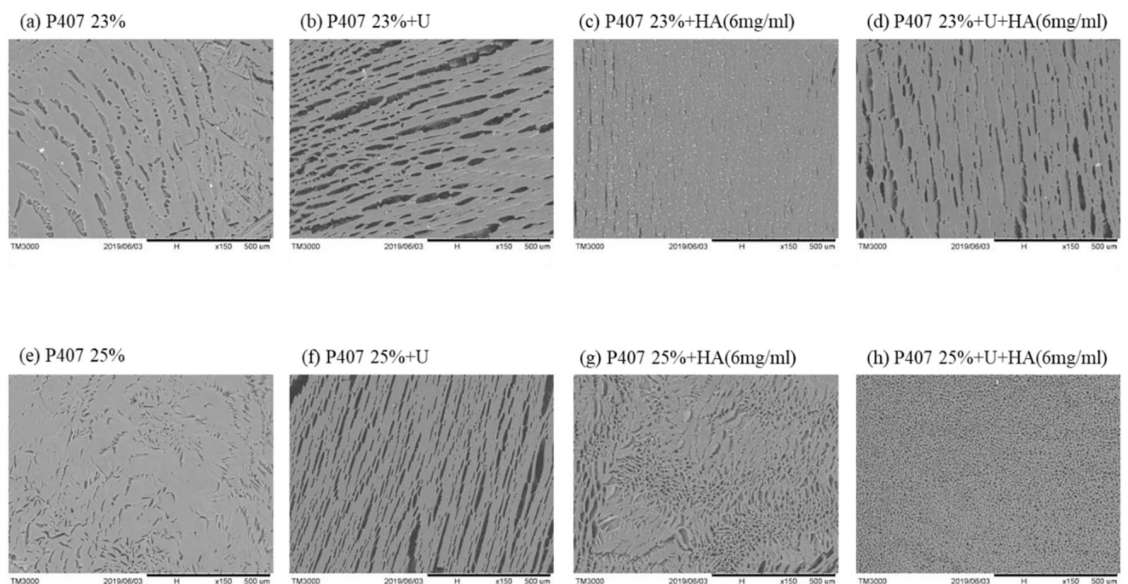

Fig 6. SEM images of the microstructure of **(a)** 23% and **(e)** 25% P407-based gels. Urokinase was added to the **(b)** 23% and **(f)** 25% P407. A more compact and porous structure was observed with an addition of 6mg HA to the **(c, g)** 23% and **(d, h)** 25% P407.

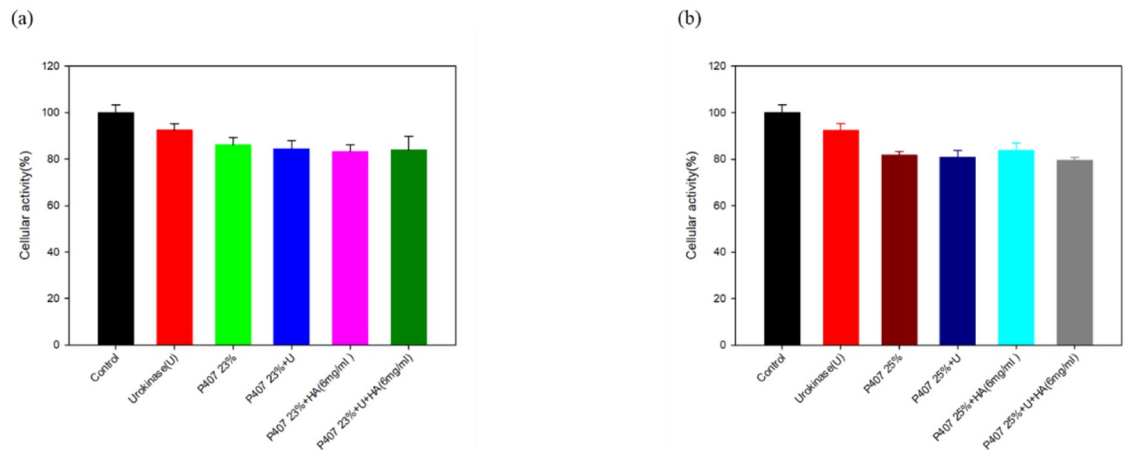https://doi.org/10.1371/journal.pone.0227784.g006

Fig 7. Alamar blue assay was used to determine the Hs68 cells cell viability. Urokinase and 6mg HA were added to **(a)**23% P407 **(b)**25% 407.

decreases as the concentration of P407 aqueous solution increases[30]. When the concentration is lower than 15% w/w, gel formation is absent regardless of the temperature change[19].

Large amount of micelles and aqueous channels make up poloxamer-based gels, making them excellent candidates to load hydrophilic molecules in spaces between micelles and channels. When the concentration of P407 is increased, a shorter inter-micellar distance and a greater tortuosity can be generated in the aqueous phase of the gel structure, resulting in more cross-links between micelles and a greater number of micelles per unit volume[31]. In spite of that, previous *in vivo* studies have explored the applicability of poloxamer-based gels and sustained delivery of model drug with the molecular weight of 5, 20, and 40 kDa. Their results implied that there is an association between high molecular weight of loaded hydrophilic drugs and faster gel erosion [19].

In our study, we observed an acceleration of gel erosion when urokinase was loaded into P407 gel. However, the addition of HA not only extended the gel dissolution time but also protected the activity of urokinase within gels, bringing forth a higher percentage of urokinase release. The acceleration of gel erosion might be attributed to the decrease in micellization intensity in the urokinase-loaded P407 gels. Adding HA into pure P407 gels also gave rise to a reduction in CMT without altering the intensity of micellization. The decrease in CMT and accelerated micellization process may represent the decrease in polarity and proportions of the hydrated methyl group in the PPO blocks[30, 32, 33]. In the context of hydrophilic drugs, gel erosion and drug diffusion occur simultaneously, which means that slower gel erosion often represents slower drug release [19, 31]. The results from our study concur with this phenomenon. In addition, our finding indicates that the existence of urokinase may result in the increase of the solubility of PPO blocks in aqueous P407 solution, possibly through formation of hydrogen bonds with the PPO blocks[34].

The addition of HA significantly postponed the event of gel erosion in the 23% P407 gels with a swelling remarkably observed. The increase in swelling of the hydrogel may occur on account of the COO^- groups within the HA/P407 hydrogels which induced the repulsive force, causing the infiltration of water infiltration and an extended process of gel erosion[24]. Although *in vitro* gel dissolution studies showed no significant increase in gel dissolution time regarding the addition of HA into the 25% P407, the swelling may not be the sole determining factor of the process of gel erosion[35–37]. We reasoned that this phenomenon is less

prominent as that in the 25% P407 gels owing to the strong inter-micellar interaction associ-
ated with the increase of P407 concentration[36].

The microstructure of poloxamer gels revealed by SEM showed that urokinase induced a
remarkable structural change with larger pore size. However, a more compact structure with
smaller pore size was observed on the HA-added poloxamer gel, which may reflect the strong
interaction between HA and poloxamer micelles. The compact porous structure also explains
the high swelling rate of P407/HA gels which was observed in the first 3 hours during the gel
dissolution[38]. This finding not only provides a good explanation of the slower erosion of
P407/HA gels, but also reveals the strong physical interactions between the two polymers[39].
Negligible cell toxicity of in vitro toxicity test was detected when 23%, 25% P407 and urokinase
were used.[40].

5. Conclusions

Our study presents a hydrogel system composed of P407 and HA that successfully achieved
sustained release of urokinase for 24 hours. Sodium hyaluronate, as an additive into P407 gels,
can decrease the CMT and accelerate the micellization process without affecting micellization
intensity and CGT. The addition of HA was found to perform better on slowing down gel ero-
sion and improving hydrogel property when mixed with aqueous P407 solution, hence result-
ing in a better regimen for longer urokinase release. HA also provides P407 hydrogel a higher
swelling property and a more compact microstructure with smaller pore size. The P407/HA
hydrogel is therefore a promising material for loading hydrophilic drugs in future given its
safe property without causing cell toxicity after local injection.

Supporting information

**S1 Fig. The Gel Permeation Chromatography(GPC) chromatogram of (A)490kDa and (B)
410kDa Hyaluronic acid(HA).**
(DOCX)

S2 Fig. Gel dissolution profiles of (a) 23% and (b) 23% urokinase-loaded P407 with HA.
The gel dissolution time decreased markedly in urokinase-loaded 23% P407 in the comparison
with the non-urokinase-loaded gels.
(DOCX)

S3 Fig. Gel dissolution profilesof (a) 25% and (b) 25% urokinase-loaded P407 with HA.
The gel dissolution time decreased markedly in urokinase-loaded 23% P407 in the comparison
with the non-urokinase-loaded gels.
(DOCX)

S4 Fig. Affidavit of approval of animal use protocol.
(DOCX)

Acknowledgments

Author Contributions

Conceptualization: Hao-Ying Hsieh, Wei-Yang Lin, Tai-Horng Young.

Data curation: Hao-Ying Hsieh.

Formal analysis: Hao-Ying Hsieh, Wei-Yang Lin.

Funding acquisition: Wei-Yang Lin, Ke-Cheng Chen.

Investigation: Hao-Ying Hsieh, Wei-Yang Lin, An Li Lee.

Methodology: Hao-Ying Hsieh, Wei-Yang Lin.

Project administration: Hao-Ying Hsieh.

Software: Hao-Ying Hsieh.

Validation: Hao-Ying Hsieh.

Visualization: Hao-Ying Hsieh.

Writing – original draft: Hao-Ying Hsieh, An Li Lee.

Writing – review & editing: Wei-Yang Lin, Yi-Chen Li, Yi-Jane Chen, Tai-Horng Young.

References

1. Ahmed A.E.H. and Yacoub T.E., Empyema thoracis. Clinical medicine insights Circulatory, respiratory and pulmonary medicine, 2010. 4: p. 1–8. https://doi.org/10.4137/ccrpm.s5066 PMID: 21157522

2. Watkins E. Jr. and Fielder C.R., Management of nontuberculous empyema. Surg Clin North Am, 1961. 41: p. 681–93. https://doi.org/10.1016/s0039-6109(16)36391-5 PMID: 13783388

3. Chan P.W., et al., Treatment of pleural empyema. J Paediatr Child Health, 2000. 36(4): p. 375–7. https://doi.org/10.1046/j.1440-1754.2000.00525.x PMID: 10940174

4. Krishnan S., et al., Urokinase in the management of complicated parapneumonic effusions in children. Chest, 1997. 112(6): p. 1579–83. https://doi.org/10.1378/chest.112.6.1579 PMID: 9404757

5. Stefanutti G., et al., Evaluation of a pediatric protocol of intrapleural urokinase for pleural empyema: a prospective study. Surgery, 2010. 148(3): p. 589–94. https://doi.org/10.1016/j.surg.2010.01.010 PMID: 20304453

6. Brandani P. and Stroeve P., Adsorption and Desorption of PEO−PPO−PEO Triblock Copolymers on a Self-Assembled Hydrophobic Surface. Macromolecules, 2003. 36(25): p. 9492–9501.

7. Ur-Rehman T., Tavelin S., and Grobner G., Chitosan in situ gelation for improved drug loading and retention in poloxamer 407 gels. Int J Pharm, 2011. 409(1–2): p. 19–29. https://doi.org/10.1016/j.ijpharm.2011.02.017 PMID: 21335076

8. Ur-Rehman T., Tavelin S., and Grobner G., Effect of DMSO on micellization, gelation and drug release profile of Poloxamer 407. Int J Pharm, 2010. 394(1–2): p. 92–8. https://doi.org/10.1016/j.ijpharm.2010.05.012 PMID: 20472044

9. Singh-Joy S.D. and McLain V.C., Safety assessment of poloxamers 101, 105, 108, 122, 123, 124, 181, 182, 183, 184, 185, 188, 212, 215, 217, 231, 234, 235, 237, 238, 282, 284, 288, 331, 333, 334, 335, 338, 401, 402, 403, and 407, poloxamer 105 benzoate, and poloxamer 182 dibenzoate as used in cosmetics. Int J Toxicol, 2008. 27 Suppl 2: p. 93–128.

10. Amiji M.M., et al., Intratumoral administration of paclitaxel in an in situ gelling poloxamer 407 formulation. Pharm Dev Technol, 2002. 7(2): p. 195–202. https://doi.org/10.1081/pdt-120003487 PMID: 12066574

11. Barichello J.M., et al., Absorption of insulin from pluronic F-127 gels following subcutaneous administration in rats. Int J Pharm, 1999. 184(2): p. 189–98. https://doi.org/10.1016/s0378-5173(99)00119-2 PMID: 10387948

12. El-Kamel A.H., In vitro and in vivo evaluation of Pluronic F127-based ocular delivery system for timolol maleate. Int J Pharm, 2002. 241(1): p. 47–55. https://doi.org/10.1016/s0378-5173(02)00234-x PMID: 12086720

13. Liu Y., et al., Effect of carrageenan on poloxamer-based in situ gel for vaginal use: Improved in vitro and in vivo sustained-release properties. Eur J Pharm Sci, 2009. 37(3–4): p. 306–12. https://doi.org/10.1016/j.ejps.2009.02.022 PMID: 19491020

14. Pillai O. and Panchagnula R., Transdermal delivery of insulin from poloxamer gel: ex vivo and in vivo skin permeation studies in rat using iontophoresis and chemical enhancers. J Control Release, 2003. 89(1): p. 127–40. https://doi.org/10.1016/s0168-3659(03)00094-4 PMID: 12695068

15. Jansen M.M., et al., Controlled release of morphine from a poloxamer 407 gel. Int J Pharm, 2013. 452 (1–2): p. 266–9. https://doi.org/10.1016/j.ijpharm.2013.05.032 PMID: 23707252

16. Li C., et al., Enhancement in bioavailability of ketorolac tromethamine via intranasal in situ hydrogel based on poloxamer 407 and carrageenan. Int J Pharm, 2014. 474(1–2): p. 123–33. https://doi.org/10.1016/j.ijpharm.2014.08.023 PMID: 25138250

17. Fasoli E., et al., Extensive heterogeneity of human urokinase, as detected by two-dimensional mapping. Anal Chem, 2015. 87(3): p. 1509–13. https://doi.org/10.1021/ac5037796 PMID: 25525926

18. Choong P.F. and Nadesapillai A.P., Urokinase plasminogen activator system: a multifunctional role in tumor progression and metastasis. Clin Orthop Relat Res, 2003(415 Suppl): p. S46–58. PMID: 14600592

19. Zhang K., et al., Poloxamer-based in situ hydrogels for controlled delivery of hydrophilic macromolecules after intramuscular injection in rats. Drug Deliv, 2015. 22(3): p. 375–82. https://doi.org/10.3109/10717544.2014.891272 PMID: 24601854

20. Fraser J.R., Laurent T.C., and Laurent U.B., Hyaluronan: its nature, distribution, functions and turnover. J Intern Med, 1997. 242(1): p. 27–33. https://doi.org/10.1046/j.1365-2796.1997.00170.x PMID: 9260563

21. Yadav A.K., Mishra P., and Agrawal G.P., An insight on hyaluronic acid in drug targeting and drug delivery. J Drug Target, 2008. 16(2): p. 91–107. PMID: 18274931

22. Hsu S.H., et al., Physicochemical characterization and drug release of thermosensitive hydrogels composed of a hyaluronic acid/pluronic f127 graft. Chem Pharm Bull (Tokyo), 2009. 57(5): p. 453–8.

23. Lee J.W., Lim T.H., and Park J.B., Intradiscal drug delivery system for the treatment of low back pain. J Biomed Mater Res A, 2010. 92(1): p. 378–85. https://doi.org/10.1002/jbm.a.32377 PMID: 19191317

24. Huh H.W., Zhao L., and Kim S.Y., Biomineralized biomimetic organic/inorganic hybrid hydrogels based on hyaluronic acid and poloxamer. Carbohydr Polym, 2015. 126: p. 130–40. https://doi.org/10.1016/j.carbpol.2015.03.033 PMID: 25933531

25. Zhang L., et al., Development and in-vitro evaluation of sustained release poloxamer 407 (P407) gel formulations of ceftiofur. J Control Release, 2002. 85(1–3): p. 73–81. https://doi.org/10.1016/s0168-3659(02)00273-0 PMID: 12480313

26. Stief T.W., In vitro Simulation of Therapeutic Thrombolysis With Microtiter Plate Clot-Lysis Assay. Clinical and Applied Thrombosis/Hemostasis, 2006. 12(1): p. 21–32. https://doi.org/10.1177/107602960601200105 PMID: 16444431

27. Sharma N., et al., Evaluation of Anticancer activity of Silver Nanoparticles on the A549 Human Lung Carcinoma Cell Lines through Alamar Blue Assay. Bio-protocol, 2019. 9(1): p. e3131.

28. Deng Y., et al., Thermodynamics of micellisation and gelation of oxyethylene/oxypropylene diblock copolymers in aqueous solution studied by light scattering and differential scanning calorimetry. Journal of the Chemical Society, Faraday Transactions, 1992. 88(10): p. 1441–1446.

29. Trong L.C., Djabourov M., and Ponton A., Mechanisms of micellization and rheology of PEO-PPO-PEO triblock copolymers with various architectures. J Colloid Interface Sci, 2008. 328(2): p. 278–87. https://doi.org/10.1016/j.jcis.2008.09.029 PMID: 18845304

30. Alexandridis P., Holzwarth J.F., and Hatton T.A., Micellization of Poly(ethylene oxide)-Poly(propylene oxide)-Poly(ethylene oxide) Triblock Copolymers in Aqueous Solutions: Thermodynamics of Copolymer Association. Macromolecules, 1994. 27(9): p. 2414–2425.

31. Bhardwaj R. and Blanchard J., Controlled-release delivery system for the alpha-MSH analog melanotan-I using poloxamer 407. J Pharm Sci, 1996. 85(9): p. 915–9. https://doi.org/10.1021/js960097g PMID: 8877878

32. Alexandridis P. and Alan Hatton T., Poly(ethylene oxide)-poly(propylene oxide)-poly(ethylene oxide) block copolymer surfactants in aqueous solutions and at interfaces: thermodynamics, structure, dynamics, and modeling. Colloids and Surfaces A: Physicochemical and Engineering Aspects, 1995. 96(1): p. 1–46.

33. Alexandridis P. and Holzwarth J.F., Differential Scanning Calorimetry Investigation of the Effect of Salts on Aqueous Solution Properties of an Amphiphilic Block Copolymer (Poloxamer). Langmuir, 1997. 13 (23): p. 6074–6082.

34. Gou M., et al., A novel injectable local hydrophobic drug delivery system: Biodegradable nanoparticles in thermo-sensitive hydrogel. Int J Pharm, 2008. 359(1–2): p. 228–33. https://doi.org/10.1016/j.ijpharm.2008.03.023 PMID: 18448286

35. Li J. and Mooney D.J., Designing hydrogels for controlled drug delivery. Nature reviews Materials, 2016. 1(12): p. 16071. https://doi.org/10.1038/natrevmats.2016.71 PMID: 29657852

36. Gratieri T., et al., A poloxamer/chitosan in situ forming gel with prolonged retention time for ocular delivery. Eur J Pharm Biopharm, 2010. 75(2): p. 186–93. https://doi.org/10.1016/j.ejpb.2010.02.011 PMID: 20188828

37. Gratieri T., et al., A poloxamer/chitosan in situ forming gel with prolonged retention time for ocular delivery. European Journal of Pharmaceutics and Biopharmaceutics, 2010. 75(2): p. 186–193. https://doi.org/10.1016/j.ejpb.2010.02.011 PMID: 20188828

38. Tuncay Tanrıverdi S., et al., Preparation and in vitro evaluation of melatonin-loaded HA/PVA gel formulations. Pharmaceutical Development and Technology, 2018. 23(8): p. 815–825. https://doi.org/10.1080/10837450.2016.1268158 PMID: 27915492

39. Mayol L., et al., A novel poloxamers/hyaluronic acid in situ forming hydrogel for drug delivery: Rheological, mucoadhesive and in vitro release properties. European Journal of Pharmaceutics and Biopharmaceutics, 2008. 70(1): p. 199–206. https://doi.org/10.1016/j.ejpb.2008.04.025 PMID: 18644705

40. Akkari A.C.S., et al., Poloxamer 407/188 binary thermosensitive hydrogels as delivery systems for infiltrative local anesthesia: Physico-chemical characterization and pharmacological evaluation. Materials Science and Engineering: C, 2016. 68: p. 299–307.